Thermal Regeneration of Fiber Bragg Gratings in Six-Hole Microstructured Optical Fibers

Dinusha Serandi Gunawardena[1], Zhengyong Liu[1,*], On Kit Law[1], Chao Lu[2], Hwa-Yaw Tam[1]
[1]*Photonics Research Centre, Department of Electrical Engineering, The Hong Kong Polytechnic University, Hung Hom, KLN, Hong Kong*
[2]*Photonics Research Centre, Department of Electronic and Information Engineering, The Hong Kong Polytechnic University, Hung Hom, KLN, Hong Kong*
**zhengyong.liu@connect.polyu.hk*

Abstract: Thermal regeneration characteristics of fiber Bragg gratings in two types of six-hole microstructured optical fibers are investigated. The difference in the air hole size of the fibers lead to different regeneration properties of the gratings.
OCIS codes: (060.3735) Fiber Bragg gratings; (060.4005) Microstructured fibers; (060.2400) Fiber properties; (060.2370) Fiber optics sensors

1. Introduction

The vast growth and usage of optical fiber sensors employed with fiber Bragg gratings (FBGs) signify their importance as sensing elements in various applications due to their intrinsic advantages which include immunity to electromagnetic interference, multiplexing capabilities, versatility, and the ability to operate in harsh environments. Owing to the structural limitations, degradation in the grating reflectivity and poor stability, in general, the operating conditions of conventional FBGs are confined to its comfort zone where the temperatures are below 300 °C [1]. However, there are many industries which require efficient functionality of FBGs at higher temperature environments such as aeronautical, oil and gas industries.

The pursuit for improved sustainability at high temperatures has involved many techniques. For instance, formation of type II [2] and type IIA [3] gratings with the use of femtosecond lasers, fabrication of optical fibers using different dopants and glass compositions [4] and quenching and annealing pre or post grating inscription [5-7]. In the last decade, a new class of gratings with pronounced sustainability at high temperatures has been discovered referred to as regenerated fiber Bragg gratings (RFBGs) [8-9]. The grating structures are regenerated and stabilized after the refractive index modulations of the seed gratings are erased during a high temperature annealing process. In attempts to enhance the thermal resistance of the gratings, several techniques of thermal regeneration have been explored. Fabrication of fibers with different dopants [10], hydrogen/helium loading [9,11], usage of ultra-short pulsed lasers [12] and CO_2 laser [13] are few of them. The superior temperature stability, considerably simple fabrication procedure and the good grating quality of RFBGs have attracted the attention of the research community. However, bulk of the FBG regeneration studies revolve around exploration of regeneration characteristics in single mode optical fibers (SMF) with different dopants/co-dopants whereas only a few have revealed the existence of RFBGs in microstructured optical fibers (MOFs) [14] thereby, increasing the need for further investigation.

MOFs with air holes in the cladding region play a vital role in the development of various types of sensors such as pressure sensors [15], gas sensors [16], refractive index sensors [17] and bio sensors [18]. In this study, we report for the first time, to the best of our knowledge regenerated gratings in six-hole microstructured optical fibers (SHMOFs) and the effect of the size of the air holes on the regenerative characteristics of these gratings. The article focuses on the evolution of the grating reflectivity, shift of the Bragg wavelength (λ_B) during the regeneration procedure and the temperature sensitivity of the two types of SHMOFs.

2. Fabrication of SHMOFs and Grating Inscription

The SHMOFs were fabricated in house using the stack-and-draw technique [19]. The SEM photos of these SHMOFs with regularly arranged six air holes, are shown in Fig. 1(a) and (b) below. The air holes of SHMOF-1

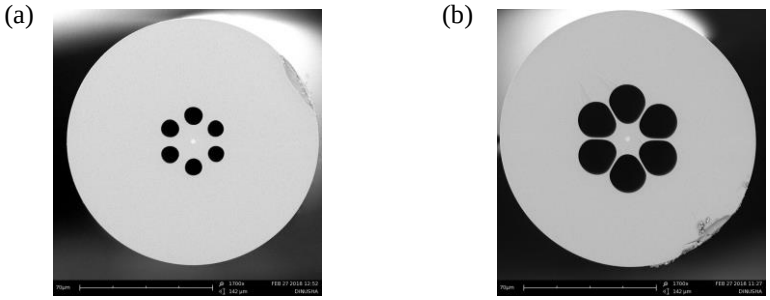

Fig. 1. SEM photos of the fiber cross section of (a) SHMOF-1 and (b) SHMOF-2

have a diameter of 11 µm and a pitch of 15 µm whereas that of SHMOF-2 are 17 µm and 18 µm, respectively. The outer diameters of the two SHMOFs are ~125 µm. During the fiber drawing process, ~40 kPa pressure was applied to collapse the small air gaps between the capillaries and rods in the stacked preform. The drawing temperature and the tension amounted to ~1960 °C and 0.5 N, respectively. A germanium-doped suspended core with a diameter of ~2 µm was introduced to both SHMOFs to facilitate modal guidance and grating inscription. 10 mm long gratings were inscribed in the SHMOFs which were H_2 loaded at a pressure of 1500 Psi for two weeks prior to the grating inscription process. A 248 nm KrF excimer laser and a phasemask with a pitch of 1065.4 nm were used in FBG inscription. After the grating inscription procedure, the SHMOFs were annealed at 80 °C for 12 hours and then left at room temperature for 14 days to remove the residual H_2 gas. The SHMOFs were then connected with SMF using a manual splicing process with the aid of a commercial fusion splicer (FITEL-S178). Since the outer diameter of the SHMOFs are ~125 µm, which is similar to that of SMF, the cladding boundaries were manually aligned and spliced afterwards using a reduced arc strength.

3. Thermal Activation of RFBGs in SHMOFs

The seed gratings of the SHMOFs were inserted into a tube furnace one at a time and placed at the center region of the furnace permitting the temperature to be uniformly distributed along the length of the seed gratings during the thermal annealing process. The temperature was increased at a ramping rate of 3 °C/min from room temperature (22 °C) until the seed gratings were completely erased at which point the temperature was held constant for 60 minutes until the RFBGs appear and completely stabilize. The reflection spectra were monitored and recorded using a LabVIEW program throughout the experiment for detailed analysis. Afterwards, a temperature calibration process was conducted on the RFBGs and repeated for two cycles to verify the validity of the obtained results. Fig. 2(a) and (b) show the evolution of the grating reflectivity and the shift in λ_B of the FBGs in the two types of SHMOFs. With increasing temperature, the seed gratings gradually extinguish until complete erasure and subsequently, the rise of RFBGs are observed at 895 °C and 910 °C for SHMOF-1 and SHMOF-2, respectively. Therefore, the SHMOF consisting of large air holes appear to possess a higher regeneration temperature compared to that of the SHMOF with small air holes. Furthermore, when compared the peak power of the seed gratings and the regenerated gratings of the two types of SHMOFs, evidently SHMOF-1 indicates a higher ratio compared to that of SHMOF-2 signifying a higher index modulation ratio, $\Delta\eta_{reg}/\Delta\eta_{seed}$ for the SHMOF with small air holes compared to that of large air holes. As illustrated in the insets of Fig. 2 (a) and (b), the decay in the grating reflectivity with increasing temperature is due to the decrease in UV induced index modulation. Moreover, the entire heating process results in a shift of ~ 12 nm and 12.5 nm in λ_B of the FBGs inscribed in SHMOF-1 and SHMOF-2, respectively until the point where the RFBGs are

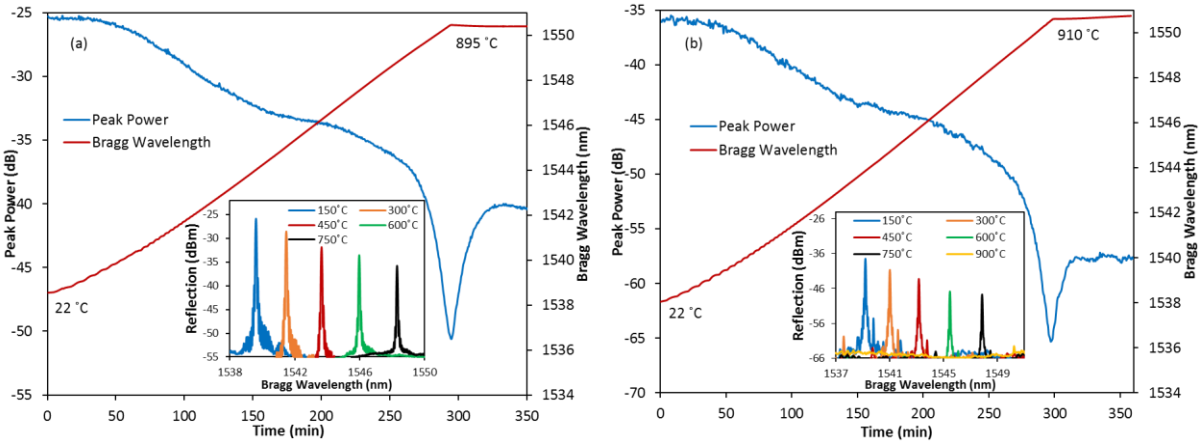

Fig. 2. Evolution of the grating reflectivity and Bragg wavelength shift during thermal regeneration (a) from 22 ˚C to 895 ˚C for SHMOF-1. Inset, reflection spectra during the thermal annealing process. (b) from 22 ˚C to 910 ˚C for SHMOF-2. Inset, reflection spectra during the thermal annealing process.

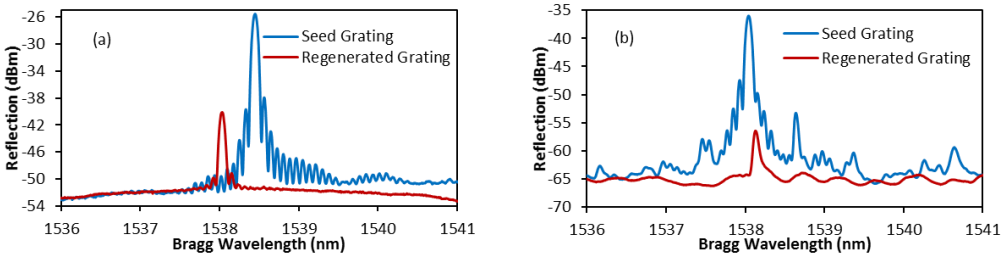

Fig. 3. Reflection spectra of seed and regenerated gratings of (a) SHMOF-1, and (b) SHMOF-2

completely stabilized. From Fig. 3(a) and (b), a noteworthy decrease in the bandwidth, the side lobes and the reflection peak power can be observed for the regenerated gratings compared to that of the seed gratings of the two types of SHMOFs, which indicates a reduction of the refractive index and the grating strength. During regeneration, the UV-induced stress in the grating is reduced to a minimum level at the regeneration temperature which is followed by a structural rearrangement of the molecular structure of the glass matrix resulting in the emergence of a new grating with superior temperature resistance and sustainability. With reference to Fig. 3(a), the blue shift in λ_B of the RFBG in SHMOF-1 can be ascribed to the relaxation of UV-induced $\Delta\eta_{DC}$. However, Fig. 3(b) indicates a slight red shift in λ_B of the RFBG in SHMOF-2 signifying the potential for the UV-induced stress and structural stress to be further reduced. The reasons responsible for this red shift is still unclear. Further experiments are currently being carried out to investigate the possible reasons for this effect.

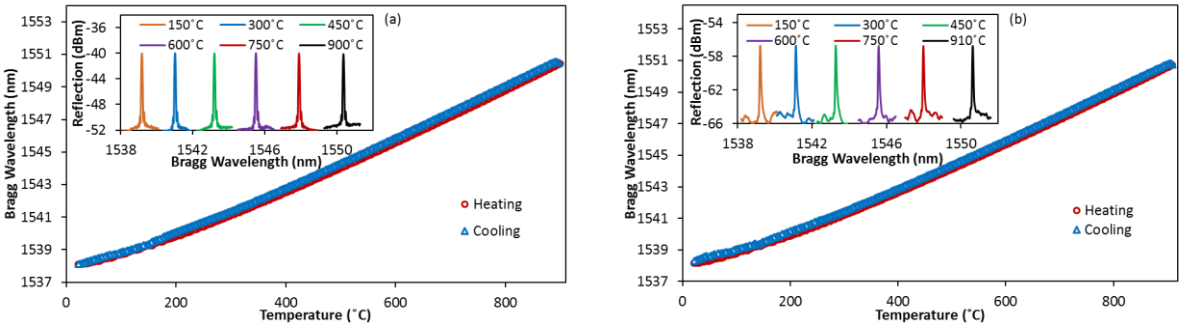

Fig. 4. First cycle of thermal calibration at a temperature ramping rate of 3 °C/min (a) for SHMOF-1 over the temperature range of 22 °C to 900 °C. Inset, reflection spectra of the RFBG of SHMOF-1 (b) for SHMOF-2 over the temperature range of 22 °C to 910 °C. Inset, reflection spectra of the RFBG of SHMOF-2.

Fig. 4(a) and (b) demonstrate the thermal calibration process conducted on the RFBGs in SHMOF-1 and SHMOF-2. In the temperature range from 250 °C to 900 °C λ_B of the RFBG in SHMOF-1 exhibits a linear function of temperature with a temperature sensitivity of 15.5 pm/°C along with the absence of any observable hysteresis. A similar behavior is observed in λ_B of the RFBG in SHMOF-2 over the temperature range from 250 °C to 910 °C with a temperature sensitivity of 15.5 pm/°C. From the insets of Fig. 4(a) and (b), it is noticed that the RFBGs successfully withstood the high temperatures since both the shape and the strength of the reflection spectra are not weakened or altered by the heating. Fig. 5 and Fig. 6 clearly illustrate the overlap in the shift of λ_B during both heating and cooling processes for two cycles indicating a similar temperature sensitivity and therefore, verify the repeatability of the experiment.

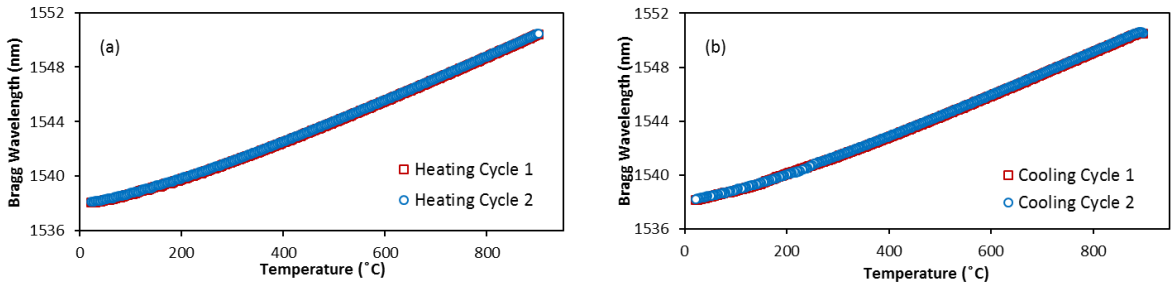

Fig. 5. Bragg wavelength shift in the RFBG of SHMOF-1 for two cycles during (a) heating and (b) cooling

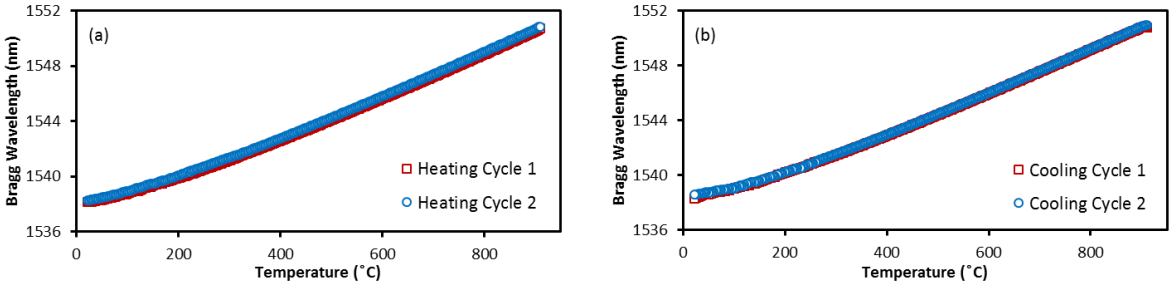

Fig. 6. Bragg wavelength shift in the RFBG of SHMOF-2 for two cycles during (a) heating and (b) cooling

4. Conclusion

In summary, we have reported thermal regeneration of FBGs in two types of SHMOFs possessing two different sizes of air holes. The SHMOF with large air holes consists of a higher regeneration temperature (910 °C) compared to that of the SHMOF with small air holes (895 °C). For fibers with core diameters as small as ~2 μm, these SHMOFs indicate superior temperature stability and therefore, are excellent candidates for high temperature sensing.

5. Acknowledgement

The authors would like to acknowledge the funding support from The Hong Kong Polytechnic University under the projects of 1-ZVGB, 1-BBYE, and 1-BBYS.

6. References

[1] S. R. Baker, H. N. Rourke, V. Baker, and D. Goodchild, "Thermal decay of fiber bragg gratings written in boron and germanium codoped silica fiber," J. Light. Technol. **15**, 1470–1477 (1997).

[2] J. L. Archambault, L. Reekie, and P. S. J. Russell, "100% reflectivity Bragg reflectors produced in optical fibres by single excimer laser pulses," Electron. Lett. **29**, 453-455 (1993).

[3] N. Groothoff and J. Canning, "Enhanced type IIA gratings for high-temperature operation," Opt. Lett. **29**, 2360-2362 (2004).

[4] O. V. Butov, E. M. Dianov, and K. M. Golant, "Nitrogen-doped silica-core fibres for Bragg grating sensors operating at elevated temperatures," Meas. Sci. Technol. **17**, 975–979 (2006).

[5] M. Åslund and J. Canning, "Annealing properties of gratings written into UV-presensitized hydrogen-outdiffused optical fiber," Opt. Lett. **25**, 692-694 (2000).

[6] K. E. Chisholm, K. Sugden, and I. Bennion, "Effects of thermal annealing on Bragg fibre gratings in boron/germania co-doped fibre," J. Phys. D. Appl. Phys. **31**, 61–64 (1998).

[7] F. K. Coradin, V. de Oliveira, M. Muller, H. J. Kalinowski, and J. L. Fabris, "Long-term stability decay of standard and regenerated Bragg gratings tailored for high temperature operation," J. Microwaves, Optoelectron. Electromagn. Appl. **12**(2), 719–729 (2013).

[8] E. Lindner, C. Chojetzki, S. Brückner, M. Becker, M. Rothhardt, and H. Bartelt, "Thermal regeneration of fiber Bragg gratings in photosensitive fibers," Opt. Express **17**, 12523-12531 (2009).

[9] S. Bandyopadhyay, J. Canning, P. Biswas, M. Stevenson, and K. Dasgupta, "A study of regenerated gratings produced in germanosilicate fibers by high temperature annealing," Opt. Express **19**, 1198-1206 (2011).

[10] D. S. Gunawardena, K. A. Mat-Sharif, M.-H. Lai, K.-S. Lim, N. Tamchek, N. Y. M. Omar, S. D. Emami, S. Z. Muhamad-Yasin, M. I. Zulkifli, Z. Yusoff, H.-Z. Yang, H. A. Abdul-Rashid, and H. Ahmad, "Thermal Activation of Regenerated Grating in Hydrogenated Gallosilicate Fiber," IEEE Sens. J. **16**, 1659–1664 (2016).

[11] K. Cook, L.-Y. Shao, and J. Canning, "Regeneration and helium: regenerating Bragg gratings in helium-loaded germanosilicate optical fibre," Opt. Mater. Express **2**, 1733-1742 (2012).

[12] K. Cook, C. Smelser, J. Canning, G. le Garff, M. Lancry, and S. Mihailov, "Regenerated femtosecond fibre Bragg gratings," Proc. SPIE **8351**, 835111 (2012).

[13] M.-H. Lai, D. S. Gunawardena, K.-S. Lim, H.-Z. Yang, and H. Ahmad, "Observation of grating regeneration by direct CO_2 laser annealing," Opt. Express **23**, 452-463 (2015).

[14] T. Chen, R. Chen, C. Jewart, B. Zhang, K. Cook, J. Canning, and K. P. Chen, "Regenerated gratings in air-hole microstructured fibers for high-temperature pressure sensing," Opt. Lett. **36**, 3542-3544 (2011).

[15] Z. Liu, L. Htein, K.-K. Lee, K.-T. Lau, and H.-Y. Tam, "Large dynamic range pressure sensor based on two semicircle-holes microstructured fiber," Sci. Rep. **8**, 65 (2018).

[16] G. Yan, A. P. Zhang, G. Ma, B. Wang, B. Kim, J. Im, S. He, and Y. Chung, "Fiber-Optic Acetylene Gas Sensor Based on Microstructured Optical Fiber Bragg Gratings," IEEE Photonics Technol. Lett. **23**, 1588–1590 (2011).

[17] A. P. Zhang, G. Yan, S. Gao, S. He, B. Kim, J. Im, and Y. Chung, "Microfluidic refractive-index sensors based on small-hole microstructured optical fiber Bragg gratings," Appl. Phys. Lett. **98**, 221109 (2011).

[18] T. M. Monro, S. Warren-Smith, E. P. Schartner, A. François, S. Heng, H. Ebendorff-Heidepriem, and S. Afshar, "Sensing with suspended-core optical fibers," Opt. Fiber Technol. **16**, 343–356 (2010).

[19] Z. Liu, C. Wu, M.-L. V. Tse, and H.-Y. Tam, "Fabrication, Characterization, and Sensing Applications of a High-Birefringence Suspended-Core Fiber," J. Light. Technol. **32**, 2113–2122 (2014).